

# Chapter 1

## Introduction

**Abstract** This chapter introduces the various topics included in the book, in subsequent chapters. As the research monograph assumes that the reader has graduate level materials science knowledge, this is not discussed in the introductory chapter here. Instead, the Introduction focuses on different types of steels, including high-strength low-alloy steel, fire-resistant structural steel, heat-resistant steel, nitride-strengthened ferritic/martensitic steel and low nickel maraging steel. Examples of application of steels in structural engineering follow, in cold-formed steel portal frame, and fire safety design and developments in fire engineering of structural steelwork. The chapter can be read independently of the rest of the book, but, with its wide referencing, is also useful in assisting in reading the in-depth chapters that follow and being referred back to. Directly referring to later chapters and sections helps with the latter.

### 1.1 High-Strength Low-Alloy Steel

In order to reduce the materials cost and improve the transportation efficiency, high-strength low-alloy (HSLA) steels are widely employed in modern car manufacturing due to their excellent strength-toughness combination and weldability (Wang et al. 2009a; Kim et al. 2002; Zhao et al. 2002). HSLA plate steels are widely used throughout the world for various structural applications. These steels combine particularly high strengths with good toughness, especially developed by the controlled hot rolling process.

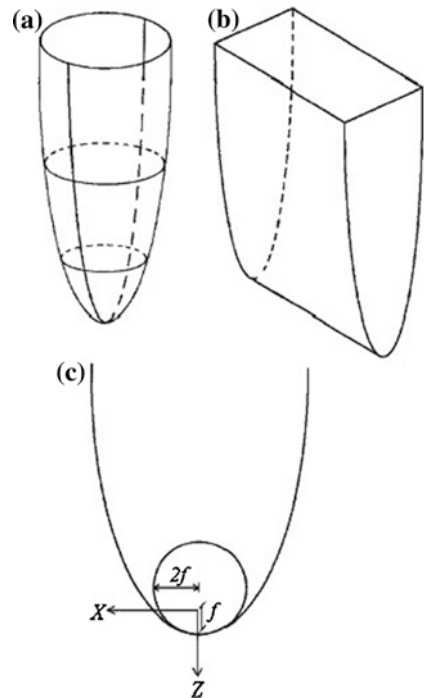
#### *1.1.1 Kinetics of Ferrite to Widmanstätten Austenite Transformation*

Various models have been developed to describe the diffusion-controlled growth of precipitates with shapes approximating to needles or plates. In the most comprehensive theory (Guo and Sha 2004a), the needle is assumed to be in the form

of a paraboloid of revolution and the plate a parabolic cylinder, Fig. 1.1a and b, respectively. The solutions obtained for specified conditions are shape-preserving when the radius of the advancing tip for either needle or plate,  $\rho$ , is several times the critical nucleus size (radius value) for plate,  $\rho_c$ , or for needle (which is twice that for plate),  $\rho_c'$ , and in this context they allow rigorously for changes in capillarity and interface kinetics as the curvature of the interface varies along the parabolic surfaces. The theory predicts a constant lengthening rate in one direction when assuming that the needle or plate tip advances into fresh parent phase.

This theory is popular because many factors that influence precipitate growth, i.e. diffusion, interface kinetics and capillarity, are accounted for within one equation, which can be solved mathematically strictly. However, the theory was developed based on many assumptions. For modelling the growth of precipitate needles or plates by diffusion of solute in solid–solid phase transformations, it assumes that interphase energy and kinetic coefficient are independent of crystallographic orientation, and neglects elastic strain energy and the anisotropy of surface properties. Nevertheless, in most solid–solid phase transformations the migration of atoms across the interface is believed to be quite rapid, so the interface kinetics effect can be neglected. Interphase energy is related to the degree of mismatch between precipitates and parent phase, which is usually anisotropic. Anisotropy of the interphase boundary structure leads to faster growth in certain directions than in others, which was not considered in the theory. In addition, the existence of the

**Fig. 1.1** Shapes used to represent needle and plate-shaped precipitates. **a** Paraboloid of revolution for needle; **b** parabolic cylinder for plate; **c** radius of the parabola tip



stress and the strain caused by the transformation will also affect the shape, or the aspect ratio, of precipitates.

In [Chap. 2](#), the effects of transformation stress/strain and anisotropic inter-phase energy on precipitate morphology are incorporated into the theory by using experimental values of the radius of the advancing tip, to study the growth kinetics of Widmanstätten austenite in ferrite in HSLA Fe–C–Mn–Nb steel. The growth theory is summarised in [Sect. 2.1.1](#).

### ***1.1.2 Change of Tensile Behaviour with Tempering Temperature***

Thermomechanical control process (TMCP) substituting for the traditional rolling process has effectively promoted the development of HSLA steels. Therefore, in recent decades the line-pipe steels have been developed from grade X60 to the current X80 and X100 grades (Koo et al. [2004](#); Asahi et al. [2004a, b](#); Fairchild et al. [2004](#)).

To achieve a combination of high strength and toughness, the microstructure of lower bainite or ferrite plus martensite is designed for HSLA steels. Hence, in spite of additions of alloying elements such as molybdenum and boron to enhance lower bainite and martensite in these steels, rapid cooling after finishing rolling is introduced. Generally, there are three cooling treatments after rolling. The first treatment is direct quenching followed by tempering (DQT). The second is accelerated continuous cooling (ACC), in which the as-rolled steel is cooled down to room temperature at a given cooling rate. The third is interrupted accelerated cooling (IAC), in which the steel is subject to water-cooling in the phase transformation temperature region, and then air-cooled to room temperature. Self-tempering could happen during air-cooling because of the slower cooling rate in the component interior. A critical point in these three cooling treatments is that the rapidly cooled steel should be tempered, which is necessary to achieve a good strength/toughness combination. However, as the lower bainite microstructure is only recently introduced in HSLA steels, studies on the mechanical properties have rarely been related to the tensile behaviour after tempering.

Tensile tests carried out on structural steels may provide valuable information related to the microstructure. In a typical tensile curve of annealed low carbon steel, the upper and lower yield points are well related to the interactions between dislocations and carbon as well as nitrogen atoms. This theory may not be able to explain the yield behaviour in other metals with fcc or hcp lattice structures. However, a convincing explanation should involve two aspects, the density of mobile dislocations and the rate of dislocation glide. The strain rate of metals is related to the value of the Burger vector,  $b$ , the mobile dislocations density,  $\rho$ , and the rate of dislocation glide,  $\bar{v}$ , as given in [Eq. 1.1](#):

$$\dot{\epsilon} = b \cdot \rho \cdot \bar{v} \quad (1.1)$$

where the rate of dislocation glide  $\bar{v}$  depends on the applied stress, as shown in Eq. 1.2:

$$\bar{v} = k \cdot \bar{v}_0 \left( \frac{\tau}{\tau_0} \right)^m \quad (1.2)$$

where  $\tau$  is the shear stress in the sliding plane;  $\tau_0$  is the shear stress for dislocation glide of a unit speed;  $m$  is the stress exponent for dislocation glide, where the rate is thermally activated. Equation 1.2 illustrates that a higher stress will produce a faster dislocation glide rate.

In the as-recrystallized state and prior to tensile loading, the mobile dislocations density may be relatively low, so a high dislocation rate is necessary to meet the demand of plastic deformation. Correspondingly, a stress peak will occur at the upper yield point on the tensile curve. Once moving, the mobile dislocations density increases quickly. Hence, a lower dislocation rate may be possible to meet the demand of plastic deformation and the stress will correspondingly decrease. Consequently, the lower yield point appears on the tensile curve. When the moving dislocations are blocked (or impeded) or re-pinned and the mobile dislocations density decreases, the same cycle described above happens again. This explanation is in principle reasonable and suitable for the plastic deformation of most metals.

Another important aspect revealed in tensile tests (and the recorded stress-strain curves) is the strain-hardening exponent. The true stress and true strain relations of homogeneous plastic deformation can be described by Eqs. 1.3–1.5:

$$s = ke^n \quad (1.3)$$

$$s = \sigma(1 + \varepsilon) \quad (1.4)$$

$$e = \ln(1 + \varepsilon) \quad (1.5)$$

where  $s$  is the true stress that can be calculated by Eq. 1.4,  $e$  is the true strain and can be calculated by Eq. 1.5,  $\sigma$  is the engineering stress,  $\varepsilon$  is the engineering strain,  $k$  is the hardening coefficient, and  $n$  is the strain-hardening exponent, which demonstrates the amount of work hardening at an incremental deformation strain. If  $n = 1$ , this shows that the material exhibits a linear work hardening characteristic. If  $n = 0$ , this indicates that the material has no strain hardening ability and behaves ideally plastic.

Section 2.3 is concerned with the tensile behaviour of HSLA steel with lower bainite microstructure after tempering at different temperatures.

### 1.1.3 Delamination Fracture Related to Tempering

Due to possible applications in severe service environments, the low temperature impact toughness is being given more attention and becomes significant to the application of HSLA steels. Therefore, the toughness at a certain low temperature is always one of the most important properties specified for HSLA

steels. In particular, their impact toughness at  $-30\text{ }^{\circ}\text{C}$  should be high enough to meet service demands. However, when the strength is very high, it becomes more difficult to achieve excellent toughness, especially at low temperatures, due to the conflict of the commonly used mechanisms for improving strength and toughness and the limited capability of manufacturing facilities. In addition, delamination, i.e. splitting in the form of single or multiple secondary cracks perpendicular to the main crack and parallel to the plate surface, is often encountered during impact fracture of hot-rolled high-strength steels (Yang et al. 2008a, b). The density of delamination usually initially increases with the decreasing temperature (Tsuji et al. 2004; Song et al. 2005, 2006), and then goes through a maximum and decreases.

The effect of delamination on impact toughness has been widely investigated on many HSLA steels such as X60, X70 and X80 pipeline steels (Wallin 2001; Silva et al. 2005, Guo et al. 2002). It has often been reported that the delamination reduced the notch impact value in the upper shelf region (Tsuji et al. 2004; Song et al. 2005, 2006; Otárola et al. 2005; Verdeja et al. 2003). On the other hand, Kimura et al. (2007), Zhao et al. (2005), and Pozuelo et al. (2006) showed that the delamination can improve toughness due to the delamination toughening effect. It will be shown in Sect. 2.4 that delamination does not seem to have much influence on the low temperature toughness at  $-30\text{ }^{\circ}\text{C}$  (Yang et al. 2008b). This point should be the subject of further study.

The initiation of the delamination in either dynamic (e.g. impact) or static conditions has not yet been sufficiently explained. From previous studies, it seems that such features as bent ferrite-pearlite microstructure, elongated grain shape, strip microstructure (Yang et al. 2008a), certain texture characteristics (Tsuji et al. 2004; Verdeja et al. 2003; Zhao et al. 2005), decohesion of grain boundaries, segregation of impurity atoms, and aligned particles (Otárola et al. 2005) and inclusions (Yang et al. 2008a) could lead to delamination, either individually (Tsuji et al. 2004) or cooperatively (Yang et al. 2008a). Although these proposed mechanisms have widely different aspects, they do have the common characteristic that the microstructures are anisotropic. Hence, it is quite natural that frequent delamination was not thought to be the result of insufficient roll-bonding after ARB (accumulative roll bonding), but rather a characteristic feature of the ultrafine elongated grain structures produced by heavy deformation (Tsuji et al. 2004).

The delamination on the fracture surfaces in Sect. 2.4 is observed on steel reheated in a certain range of temperature after rolling. In Sect. 2.4, the delamination is described in detail and their effect on the low temperature toughness at  $-30\text{ }^{\circ}\text{C}$  is evaluated. The relationship between delamination and the microstructural changes resulting from the reheating is described.

## 1.2 Fire-Resistant Structural Steel

Steel is the most important metallurgical material available to civil engineers worldwide. Interest in the area of fire resistance of steel for safety and economy has grown in the last two decades. The development of fire-resistant steels is one

aspect of the effort to enhance building safety in fire. This effort has been mainly from Nippon Steel, where some fire-resistant steels have been developed containing niobium and/or molybdenum. These steels have increased yield strength at elevated temperatures, believed to be especially for meeting the requirements of Japanese building regulations.

Traditionally, fire resistance of steel building structures is achieved by applying fire protection to steel columns and beams. However, fire engineering has been rapidly developed and one aim has been to design buildings with significant built-in fire resistance via the use of reduced or no traditional fire protection.

A further approach towards ensuring fire safety of steel structures is the use of a fire resistant-type structural steel in construction. This term 'fire resistant steel' simply refers to a structural steel that has better strength performance at elevated temperatures, typical of those that a steel section in a building would experience in a fire. Using such steel would not complicate current design routines significantly, as only new strength reduction factors or limiting temperature tables would need to be used in fire design calculations. Microalloyed steel of this nature, with elevated temperature properties, is well established in the boiler and superheated market areas. At present, however, these steels while technically possible, are not available in the general construction market, nor would they be economically competitive with established and readily available systems.

The driving force for the development in Japan of structural steels with fire resistant microstructures was the Japanese construction standards. They are stricter than Western standards and restrict the maximum steel temperature to the temperature at which the steel retains two-thirds of its room temperature yield strength. A number of fire-resistant steels so named by the Japanese steel manufacturers have found use in the Japanese market. These, and other developments of such steels, were reviewed in an overview paper (Sha et al. 2001) that includes extensive references.

In Japan, a significant amount of research has been carried out by Nippon Steel, where several fire-resistant steels have been developed. These steels represent a notable improvement over conventional steels, judging by the Japanese 'New fire safety design system', which allows the maximum permissible steel temperature to be set in terms of elevated temperature yield strength. However, their advantage is limited, as Eurocodes, and other building standards in the West do not use this parameter in design. Broken Hill Proprietary Co. (BHP) in Australia carried out earlier research on fire-resistant steels.

The author has carried out a programme of research to develop fire-resistant steels for building construction. Comprehensive microstructural characterisation and mechanical testing have been carried out on two Japanese fire-resistant steels made by Nippon Steel. The chemical compositions of these steels are given in Table 3.1. The research has shown that there is a strong relationship between the relatively high elevated temperature tensile strength and fine precipitation as well as coarse inclusion particles. The good high temperature strength and creep properties of Nippon steels are owing to the high lattice friction stresses. These are a result of the very fine distribution of precipitates with limiting theoretical carbide

having a composition of MX where X is nitrogen and/or carbon, molybdenum in solid solution and a strong secondary wave of precipitation at approximately 550 °C. Here, the term ‘lattice friction stress’ should be regarded as the inherent resistance of an iron crystal structure to dislocation motion plus the hardening effect of solutes, precipitates and dislocations. This lattice friction stress maintains strength up to 600 °C when grain boundary sliding begins.

The effectiveness of using these fire-resistant steels in building floor construction has been evaluated, based on established fire test data and the current codes of standard. It has been found that they can achieve a relatively small gain in ‘hot’ moment resistance and the load ratio that a steel structure can withstand in fire. It has also been found through the calculations that, in order to achieve a 30-min increase in fire resistance in conventional composite floor structures, the steel is required to retain its strength at 150 °C higher than conventional commercial structural steels.

Several experimental fire-resistant steels have been designed (Chap. 3), to test the effectiveness of two methods devised by the author for achieving better fire performance. The first is to react to the high temperature reached in a fire by precipitation, which leads to in situ strengthening. The second is to rely on the steel’s thermal stability to provide good elevated temperature strength. These steels can provide better fire resistance than conventional structural steels.

Chapter 3 describes the microstructural characterisation and the mechanical properties of the fire-resistant steels. The control materials are the two Nippon steels and the conventional S275 steel (designation used in Eurocodes) formerly known as grade 43 steel (designation used in British Standards). Detailed analyses on these steels are presented.

Further to the literature reviewed by Sha et al. (2001), additional new experimental fire-resistant steels were developed (Chap. 3). Sections 3.3 and 3.4 describe and discuss atom probe field ion microscopy work on two examples of Japanese commercial steels and two experimental steels developed at Queen’s University Belfast. The research will be compared with that obtained with a multiple of other, more conventional techniques Sha et al. (2001) and the references quoted in it and in Chap. 3. An overview of the behaviour of structural steels at elevated temperatures and the design of fire-resistant steels, which forms a general presentation of the background of Chap. 3, are given elsewhere by Sha et al. (2001) and will not be repeated here.

### 1.3 Heat-Resistant Steel

To save the non-recycled energy source and reduce the CO<sub>2</sub> emission requires improving the efficiency of fossil power plants, which can be achieved by developing super critical power plants. The 9–12 %Cr ferritic/martensitic heat-resistant steels have been widely used in ultra super critical (USC) power plants because of the high thermal conductivity, low thermal expansion coefficient and low susceptibility to thermal fatigue (Masuyama 2001).

The high chromium ferritic/martensitic heat-resistant steels are replacing the austenitic stainless steels as an alternative structural material for USC power plants over recent years due to their excellent mechanical properties and low cost. The main advantages of these kinds of steels include improvement of oxidation and corrosion resistance as well as long-term creep rupture strength, which mainly relies on the innovation and optimisation of the chemical composition. The chromium content was increased to enhance the oxidation and corrosion resistance and to meet the demand of the increasing operating steam temperature (Wang et al. 2009b). Addition of tungsten or substitution of tungsten for molybdenum (Miyata and Sawaragi 2001) was found beneficial to improve the creep rupture strength. Cobalt was added to balance the chromium equivalent and suppress the  $\delta$ -ferrite which is detrimental to creep rupture strength during the high temperature normalising process (Yamada et al. 2003). Over these years, steels with C–Cr–W–Co as main alloying elements have been paid increasing attention for their excellent creep resistance performance (Abe et al. 2007a; Toda et al. 2003). It was found that the creep resistance is proportional to the tungsten content in the range of 1–4 wt%. In addition, cobalt has been found to make a great contribution to creep rupture strength due to its three effects: (1) suppressing  $\delta$ -ferrite (Yoshizawa and Igarashi 2007; Yamada et al. 2003); (2) possible effect of inhabiting the coarsening of  $M_{23}C_6$  carbides (Gustafson and Ågren 2001); and (3) increasing the atomic binding forces (Li et al. 2003).

However, recent research shows that the microstructure stability of the 9–12 % Cr ferritic/martensitic heat-resistant steels is the most critical issue to the creep rupture strength in the long time service. How to improve the microstructure stability has been recognised as a key issue in developing steels with high creep rupture strength (Kimura et al. 2010). On the one hand, tungsten was found to prevent the migration of martensitic laths (Abe 2004). On the other hand, tungsten was discovered to facilitate the formation of large-size Laves phase and harmful to the microstructure stability (Abe 2001). In addition, cobalt seemed to accelerate the precipitation of tungsten, resulting in the quick coarsening of Laves phase, which will initiate creep cavities (Cui et al. 2001; Lee et al. 2006).

In addition to creep resistance, the oxidation resistance at elevated temperature is an important issue for heat-resistant steel and it can be improved by raising the chromium content in the steel. However, chromium is the main element in forming Z phase (Danielsen and Hald 2009; Golpayegani et al. 2008), which would result in deterioration of the creep rupture strength (Sawada et al. 2006b, 2007). Moreover, the driving force of Z phase formation has already been reported to depend on the chromium content in high chromium ferritic steels (Danielsen and Hald 2004). Considering these aspects, appropriate chromium content is needed to achieve a balance between oxidation-resistance and creep-resistance properties.

In Chap. 4, based on the chemical composition of ASME-P92, through tungsten and cobalt addition, a 10Cr ferritic/martensitic steel is designed. The creep-resistance property of the steel and its microstructure evolution during high temperature creep are shown. The aim of this chapter is to develop some basic idea of improving microstructure stability from the view of chemical composition and contribute to the development of advanced high chromium heat-resistant steels superior to ASME-P92 steel in both oxidation-resistance and creep-resistance properties.



## 1.4 Nitride-Strengthened Ferritic/Martensitic Steel

### 1.4.1 *Reduced Activation Ferritic/Martensitic Steels and Effect of Carbon Reduction*

Reduced activation ferritic/martensitic (RAFM) steels have been regarded as candidate structural materials of future fusion and fission power reactors. Compared to austenitic stainless steels, the RAFM steels have not only good mechanical properties and thermal conductivity, but also excellent resistance to void swelling. The present RAFM steels, Eurofer 97 (the European reference material), JLF-1 (among the Japanese Low activation Ferritic steel series), F82H, 9Cr-2WVTa (Fe-9Cr-2W-0.25V-0.12Ta-0.1C) and CLAM (Chinese Low Activation Martensite), are alloyed with chromium, tungsten, manganese, vanadium, tantalum, carbon and nitrogen (Baluc et al. 2007b), and developed in Europe, Japan, US and China. India also has fabricated RAFM steels and oxide dispersion strengthened (ODS) (Wong et al. 2008; Saroja et al. 2011). All these steels are strengthened by both solution hardening and precipitation hardening. Solution hardening of these steels is dependent on the addition of chromium and tungsten whereas precipitation hardening relies on precipitates such as  $M_{23}C_6$ , where M is mainly Cr with substitution of Fe and MX (M = V, Ta; X = C, N) carbonitride. It is well known that coarsening of precipitates during creep results in an increase in inter-particle distance, but the precipitation strengthening effect is inversely proportional to this distance; therefore, the creep rupture strength would decrease eventually. Different precipitates have different coarsening rates. Sawada et al. (2001) found that the coarsening rate of  $M_{23}C_6$  carbide is much higher than that of the MX type precipitates. Therefore, optimal control of the carbon content may be an effective method to improve the creep rupture strength of RAFM steels through changing carbides to nitrides or carbonitrides. Taneike et al. (2003) studied the creep-resistance property of the steels with different carbon contents and found that the time to rupture could be significantly increased by reducing the carbon content to a very low level, which was attributed to the elimination of carbides and the formation of fine, thermally stable and homogeneously distributed carbonitrides or nitrides in the microstructure. Much work has been carried out on the nitride-strengthened high chromium ferritic/martensitic heat-resistant steels used as structural materials for USC power generation (Taneike et al. 2004; Yin et al. 2007; Yin and Jung 2009; Abe et al. 2007b; Toda et al. 2005; Sawada et al. 2004). However, the development of nitride-strengthened RAFM steels has been limited. In Chap. 5, the microstructure and mechanical properties of the nitride-strengthened RAFM steels with higher creep rupture strength are discussed.

In these steels, both molybdenum and niobium are removed and replaced by tungsten and tantalum in order to obtain the low activation property. The typical microstructure of these heat-resistant steels is composed of tempered lathy martensite with precipitates dispersed in the matrix (Ghassemi-Armaki et al. 2009). These precipitates are of great importance to the microstructure stability. However, some work (Maruyama et al. 2001; Gustafson and Ågren 2001) (Sects. 5.1 and 5.2)

has shown that with increasing service time, the  $M_{23}C_6$  carbide grows too fast to pin the dislocation movement and cannot prevent grain boundaries or lath boundaries from migrating, resulting in premature fracture. Seeking thermally stable particles to achieve a highly stable microstructure has always been a goal in developing heat-resistant steels. Oxides such as fine  $Y_2O_3$  and  $YTiO_3$  have impressive thermal stability and could prevent the microstructure from degradation. Thus, ODS steels such as Eurofer 97-ODS and CLAM-ODS steels have been developed (de Castro et al. 2007; Olier et al. 2009; Klimenkov et al. 2009). However, the microstructures of ODS steels are usually anisotropic due to the manufacturing process and their ductile–brittle transition temperatures (DBTT) are very high (Lindau et al. 2005; Kurtz et al. 2009), though the steels showed better thermal stability (Schaeublin et al. 2002; Yu et al. 2005). Meanwhile, the fabrication involves the complicated and expensive process of powder alloying. It will be very difficult to put the ODS steels into industrial-scale practice.

Besides oxides, nitrides are also thermally stable. For a metal element, its nitride has a slower growth rate than its carbides under the same condition (Yong 2006). It was found by Taneike et al. (2003) that  $M_{23}C_6$  carbide was suppressed in the 9 %Cr martensitic steel when carbon content was reduced to as low as 0.018 % (wt%) whereas the nitrides were stimulated to homogeneously disperse, which greatly improved the microstructure stability and enhanced creep strength. In order to eliminate the  $M_{23}C_6$  carbide, Taneike et al. decreased the carbon content to even below 20 ppm and developed the totally nitride-strengthened martensitic steel. In this steel, no  $M_{23}C_6$  was precipitated, and MX nitrides distributed along the grain boundaries and lath boundaries (Abe et al. 2007b; Taneike et al. 2004). The nitride-strengthened martensitic steel showed excellent creep property at elevated temperature because of the high thermal stability of nitrides.

It is well known that a single-phase microstructure should be beneficial for steels to achieve high creep strength. However, when the carbon content is reduced to an extremely low level, if no other composition change is made,  $\delta$  ferrite will inevitably form (Sects. 5.1, 5.2, 5.3), which is harmful to both toughness and creep resistance by acting as the weak part during creep (Ryu et al. 2006; Yoshizawa and Igarashi 2007). Therefore, composition design should consider  $\delta$  ferrite elimination. Taneike et al. added 3 % cobalt to suppress  $\delta$  ferrite. Nevertheless, unlike the ordinary martensitic heat-resistant steels, the reduced activation martensitic steels cannot contain cobalt due to its negative effect on the reduced activation property. However, it is interesting to notice that manganese and cobalt are both adjacent to iron in the periodic table of elements and it is possible that manganese can be used to suppress  $\delta$  ferrite in RAFM steel. Therefore, the nitride-strengthened reduced activation martensitic steel may be developed by reduction of carbon and proper addition of manganese.

The nitride-strengthened reduced activation martensitic steel is novel and literature reports have been scarce. In Sects. 5.4, 5.5, 5.6, the possible changes of microstructure and mechanical properties with decreasing carbon content are investigated. Some special characteristics caused by carbon reduction are demonstrated.

The eventual target of the alloy development in terms of property levels is defined in the published work in this area (van der Schaaf et al. 2000; Klueh et al. 2000, 2002; Jitsukawa et al. 2002; Baluc et al. 2007a). In most of the papers, the target mechanical properties were expected to be comparable or better than 9Cr-1Mo tempered martensitic steels and the target for induced activity level was indicated. In addition, expected service condition of RAFM steels was described (Baluc 2009). The target level of toughness after irradiation was indicated (Jitsukawa et al. 2009). 9CrWVTaN martensitic steels were introduced (Klueh 2008).

In relation to the target performance of the development of the steels, the expected operation temperature under service condition of most 7-12Cr martensitic steels ranges from 300 to 550 °C. Toughness degradation by irradiation at temperatures below 400 °C would be one of the biggest issues for the development of the steels. Therefore, higher toughness is required even before irradiation.

Improvement of high temperature strength is another direction of the development. Increasing the upper temperature limit above 600 °C (up to 700 °C) has been attempted (Kurtz et al. 2009; Klueh 2008; Klueh et al. 2007; de Carlan et al. 2004). Tempering temperature of those steels was 750 °C or even higher. The tempering temperature being comparable or lower than the expected operation temperatures can lead to unstable microstructure during service.

Information about steel competitors is given above. The new steels described in Sects. 5.4, 5.5, 5.6 however, are experimental steels, as parts of a large programme of steel development. As such, further refinement in composition and processing is expected. The aim of Sects. 5.4, 5.5, 5.6 is to provide a basis for future development of steels, and to contribute to our materials science understanding of the materials, by using 9Cr base steels with two different carbon contents.

### ***1.4.2 Impact Toughness***

The efficiency of power plants could be improved by enhancing the steam parameter. At present, heat-resistant steels for the high steam parameter of 650 °C are being developed. This has put heat-resistant steels such as T/P91, T/P92 and E211 out of consideration because of the loss of the microstructure stability during service at the high temperature (Weisenburger et al. 2008). More advanced steels should be developed to meet this requirement.

It is well accepted in heat-resistant steels that highly stable microstructure will produce excellent creep strength. The precipitates are basically  $M_{23}C_6$  and MX, the carbonitride of Nb, V or Ti. The MX-type carbonitrides show much better stability than the  $M_{23}C_6$  type carbide. In order to achieve microstructure with high stability, stable precipitates such as MX-type carbonitrides are expected in heat-resistant steels.

In addition to this initial tempered martensitic microstructure, long-term microstructure stability requires attention. Such coarse precipitates as Laves phase

(Fe<sub>2</sub>W or Fe<sub>2</sub>Mo) and Z phase ((Cr,Nb)N) should be delayed, although they could only form after a long service time (Sawada et al. 2006a). The formation of Laves phase and Z phase is a thermally automatic process which cannot be avoided (Shen et al. 2009). However, this process can be delayed by reducing the content of tungsten, molybdenum and nitrogen.

Nitride-strengthened martensitic heat-resistant steel is developed, based on the above ideas. Following the alloy design and the mechanical properties of the nitride-strengthened martensitic steels, Sect. 5.7 will present the excellent impact toughness of the steel after tempering.

## 1.5 Low Nickel Maraging Steel

Maraging steels, a special class of ultrahigh strength steels simultaneously with good toughness, are martensitic hardenable alloys (Guo et al. 2004). Maraging steels are hardened by precipitates and they differ from other steels hardening by carbon (Sha and Guo 2009). The term ‘maraging’ refers to age hardening in a low carbon, iron-nickel lath martensite matrix. The precipitation hardening is due to the formation of precipitates referring to the hardening phases of intermetallic compounds between nickel and molybdenum, nickel and titanium or other additional alloying elements with nickel, or other element combinations. After precipitation hardening, the steel properties are improved significantly, characterised by high tensile strength combined with high toughness and good weldability and malleability.

Maraging steels were developed for special purposes, where the combination of high strength and good toughness was required. Maraging steels have long been regarded as excellent materials and have been applied widely for decades, in industries, e.g. aircraft, aerospace and tooling applications, due to their good machining properties (Sha and Guo 2009; Guo and Sha 2004b).

Commercial maraging steels have sufficiently high nickel content (mostly 18 wt%) to produce martensite following air cooling to room temperature upon solution treatment (Sha and Guo 2009). Nickel has been widely used in maraging steels. The advantages are that nickel raises the yield strength of iron, but also lowers the DBTT (cleavage) of iron, so it is an alloying method of raising strength and increasing toughness. However, the high nickel content has cost implications, leading to the application of these steels being largely restricted to specialised sections such as aerospace. This has generated attempts to develop alternative compositions giving equivalent properties at reduced cost.

Numerous studies have focused on developing steels with low nickel and cobalt contents, as nickel and cobalt are costly and highlighted as strategic alloying elements. Developing novel maraging steels with low nickel and cobalt contents is necessary. There was a tremendous increase in cobalt price in the 1970s, which promoted the development of cobalt-free maraging steels (Leitner et al. 2010). The development of maraging steel with 18 wt% nickel and cobalt-free was a remarkable achievement (Teledyne Vasco and Inco, USA). Subsequently, the

content of nickel was reduced to 14 wt%, cobalt-free. Another example of these further developments was the PH 13-8 Mo types (Guo et al. 2003).

Chapter 7 looks into further developing a low nickel content maraging steel, which should have reduced cost. The high cost of nickel demands second thoughts about the actual amounts required of this element in these steels and restricts the areas of application as well, since high cost materials are not suitable for general application, like in civil construction.

Table 1.1 shows the compositions of existing and developmental maraging steels and their approximate alloy costs per tonne. Alloy savings of about £2400 per tonne are possible on 12 % nickel steels compared with standard 18 % nickel steel, and about £800 per tonne on 12 % nickel steels compared with standard cobalt-free 18 % nickel steel. The alloy costs shown in Table 1.1 are based on recent prices in the UK for pure metals and therefore are for illustrative purpose only, because, obviously, metal prices change with time and place.

In order to achieve a better understanding of the function of nickel in maraging steels, the Fe-12.94Ni-1.61Al-1.01Mo-0.23Nb (wt%, for all compositions in this book unless otherwise specified) maraging steel is investigated in Chap. 7. The eventual aim of the research is to develop novel grain refined maraging steels with reduced nickel content, for high strength applications with good toughness at a reduced steel cost. The objectives are to complete mechanical testing and microstructural characterisation of the maraging steel. The main contribution would relate to commercially viable steels. Table 1.2 highlights the difference between the philosophy and the previous research (Howe 2000; Morris et al. 2000; Leinonen 2001; Priestner and Ibraheem 2000) in developing high strength steels.

X-ray diffraction analysis will be used to evaluate the formation of retained or reverted austenite. The hardness will be shown both before and after ageing treatment and then the hardness curve is determined. The toughness is measured by Charpy impact testing. One primary aim is improving toughness of this kind of maraging steel through a lower austenitisation temperature and intercritical annealing.

## 1.6 Cold-Formed Steel Portal Frame

The majority of portal frames use conventional hot-rolled steel sections for the primary load carrying members (i.e. columns and rafters) and cold-formed steel for the secondary members (i.e. purlins, side rails and cladding). Using hot-rolled steel, spans

**Table 1.1** Estimation of alloy cost made with pure metal prices

Composition	Approximate cost per tonne
Fe-18Ni-3.3Mo-8.5Co-0.2Ti-0.1Al	£3807
Fe-18.5Ni-3Mo-0.7Ti-0.1Al	£2212
Fe-12.94Ni-1.61Al-1.01Mo-0.23Nb	£1400

**Table 1.2** The novelty and contribution of the research

This research	Previous research
Improve toughness but with fair strength	Improve strength but retain fair toughness
Refine grain size → ageing treatment → use	Refine grain size → use (Howe 2000)
Achieve fine (<5 μm) grain	Achieve ultrafine (~1 μm) grain (Howe 2000)
Reduce cost by using cheaper alloying elements	Reduce cost by choosing the most economical processing routes (Morris et al. 2000; Leinonen 2001; Priestner and Ibraheem 2000)

of up to 60 m can be achieved. On the other hand, for frames of more modest spans, the use of cold-formed steel for the primary load carrying members (i.e. columns and rafters) should be a viable alternative to conventional hot-rolled steel.

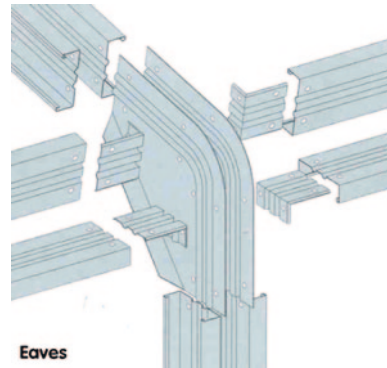
For buildings of modest span of up to 30 m, cold-formed steel portal frames (see Fig. 1.2) are an increasingly popular form of construction, particularly in Australia and the UK, and are typically used for low-rise commercial, light industrial and agricultural buildings. Such buildings use cold-formed steel channel-sections for columns and rafters, with joints formed through back-to-back gusset plates bolted to the webs of the channel-sections (see Fig. 1.3).

In the practical design of cold-formed steel portal frames, involving use of sections from one cold-formed steel manufacturer, an economical design can be achieved by selecting the appropriate sections for column and rafter through a number of different permutations of channel-sections. This is feasible since each cold-formed steel manufacturer would only have a discrete number of section sizes in their catalogue. More importantly, the parameters relating to configuration and topography of frame (frame pitch and frame spacing) are usually considered to be fixed.

However, the topography of the frame (frame pitch and frame spacing) plays a key role in the overall structural response. Therefore, the determination of these parameters, in conjunction with the selection of the cold-formed steel sections as described above, can achieve an efficient, cost-wise, building. The research

**Fig. 1.2** Cold-formed steel portal framing system

**Fig. 1.3** Swagebeam eaves joint



described in [Chap. 9](#) will concentrate on optimising the portal frame topography, with the objective function being the minimum cost per metre length of building.

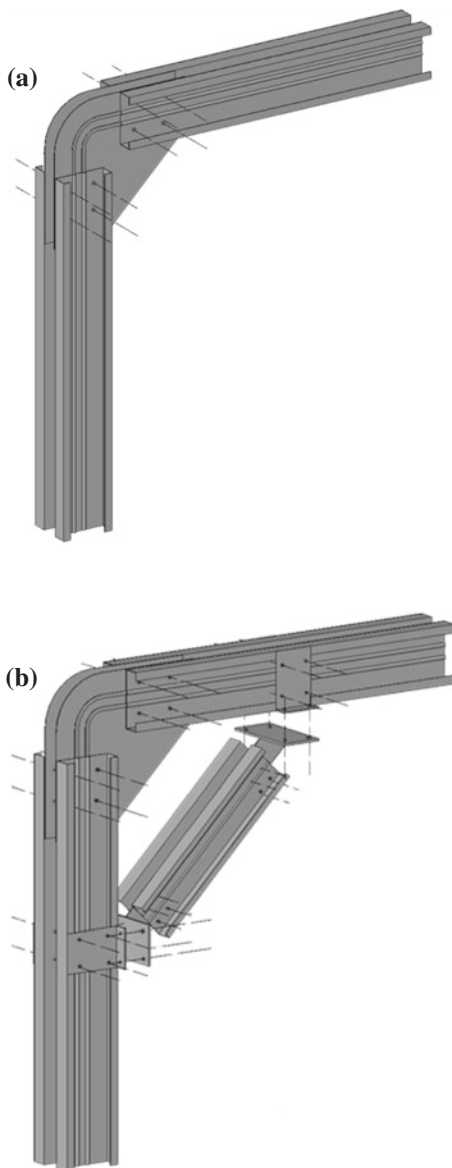
Because fabrication and erection costs for cold-formed steel are much lower than for hot-rolled steel, there is scope to vary the frame spacing and pitch. Other advantages of cold-formed steel portal frame systems compared to hot-rolled steel portal frames are as follows ([Lim and Nethercot 2002](#)). Pre-galvanised cold-formed steel sections that do not require painting to prevent rusting are maintenance-free. The transportation costs are lower due to efficient stacking of cold-formed steel sections. Also, the acquisition costs are lower as the cold-formed steel used for the secondary members can be purchased from the same manufacturer/supplier.

For such frames, moment-resisting joints at the eaves and apex can be formed through mechanical interlock (see [Fig. 1.4a](#)). As can be seen, the joints are formed through brackets that are bolted to the webs of the channel-sections. Under moment, the matching swages in both the brackets and the webs of the channel-sections interlock, thus forming a rigid joint. With longer span frames, to reduce the section sizes of both the column and rafter members, a knee brace is often included at the eaves (see [Fig. 1.4b](#)). The effect of including a knee brace is that the bending moment that needs to be resisted by both the column and rafter around the joint is reduced with the axial load carried through the knee brace ([Rhodes and Burns 2006](#)).

Over the past three decades, the design optimisation of structures has attracted much attention from researchers ([Gero et al. 2005](#)). Many structural engineering design problems have discrete decision variables. For instance, in the design of steel frames, the section sizes of the columns and rafters are selected from standard tables. One of the most efficient methods for solving complex combinatorial optimisation problems such as the design of steel portal frames is genetic algorithms (GAs), based on the Darwinian principle of survival of the fittest and adaptation.

Binary-coded GAs have been applied to the design of hot-rolled steel frames to find the discrete section sizes for the members that minimise the weight of the structure ([Kameshki and Saka 2001](#); [Toropov and Mahfouz 2001](#); [Gero et al. 2006](#)). However, one of the limitations of binary-coded GAs is the extra computational complexity of the algorithm associated with continuous decision variables

**Fig. 1.4** Details of eaves joint arrangements. **a** Mechanical interlock; **b** knee brace



(Deb 2001). Therefore, real-coded GAs (Deb 2001; Deb and Gulati 2001) were proposed to resolve the drawback of binary coded GAs.

In design optimisation of hot-rolled steel portal frames, Saka (2003) described a binary-coded GA to minimise the weight of a portal frame through selecting the most appropriate hot-rolled steel section sizes for the columns and rafters, from a catalogue of available standard sections, based on elastic analysis and



design as described in the British Standards (BS 5950-1). More recently, Issa and Mohammad (2010) described a GA using binary strings, to study the same problem. They varied the length and depth of the haunched part of the rafter in a specified range using fixed intervals to determine the optimum size of the haunched member. Hernandez et al. (2005) proposed an optimum design software named PADO, based on mathematical programming, to optimise the design of a hot-rolled steel portal frame in accordance with the Spanish code of practice (EA-95). Chen and Hu (2008) used GAs to optimise hot-rolled steel portal frames having tapered members, according to the Chinese specification for portal frames (CECS-102).

Previous research focused on the design of hot-rolled steel portal frames with fixed topology where the pitch and frame spacing were not optimised and were specified *a priori*. In Chap. 9, a GA is proposed to minimise the cost of cold-formed steel portal frame buildings by minimising the cost of the main structural elements per unit length of the building. Although any code of practice can be used the Australian code was adopted, since in Australia the spans of the frames can be larger as there is less snow.

The optimisation method addresses all the relevant combinations of the permanent and imposed loads, incorporates the full range of design constraints and considers all feasible wind load combinations. It is assumed here that full lateral restraint is applied to columns and rafters. Also, it is assumed that the cost of the purlins, side rails, and sheeting is independent of frame spacing. The research in Chap. 9 differs from the previous work on hot-rolled steel portal frames in that the section sizes of the columns and rafters and the topology of the building, including the pitch and frame spacing, are all optimised simultaneously. The decision variables used in the design optimisation are the spacing of the frames, the pitch of the roof and the section sizes of the main structural elements. Self-evidently, the solution space has both discrete and continuous variables. Also, unlike previous research on hot-rolled steel frames that used binary coding for the GA, real coding is used in Chap. 9.

## 1.7 Fire Engineering

To comply with the building regulations, fire safety design is a necessary measure. In general, fire protection of buildings can be divided into two types of measures, active and passive. The active measure is concerned with the detection and extinction of fire at its early stage, achieved by introducing alarm, control of smoke and other hazardous elements, in-built fire fighting or control and other fire safety management systems. The passive measure of fire safety design is mainly concerned with the structural fire protection and means of escape in case of fire. This can be achieved by means of enhancing structural performance including the use of fire-protected beams and columns, compartmentation, control of flammability of the structural fabric and provision of fixed escape routes.

Fire engineering is a passive measure towards fire safety for building structures. Traditionally, provision of protective material to steel columns and beams has been used to achieve fire resistance in steel structures. Fire protection is

prescriptive in that the engineer designs the steel structure based on its full strength, and then determines the fire protection required by using pre-defined charts and tables depending on the specified fire resistance. The alternative passive measure, fire engineering, is to analytically design the steel structures by using the properties and behaviour of steel at high temperature. This type of passive measure is more economical in that the needs for fire protection may be minimised or eliminated.

The development of fire engineering based on the analytical approach has resulted in steel structures that have built-in fire resistance such as slim, also called shallow, floor beam construction. Two types of slim floor beams have been developed by British Steel (now Tata Steel) and The Steel Construction Institute (SCI), UK, the fabricated Slimflor beam and the asymmetric Slimflor beam, the Slimdek. In addition, Top-Hat beam was developed in Scandinavia (Chaps. 10 and 11). The Slimflor system consists of a Slimflor beam and either pre-cast floor slab with in-fill concrete or composite construction with deep decking. The composite Slimdek system is constructed using an asymmetric Slimflor beam (ASB) with deep decking. Another option of fire engineering in steel structures is to use fire-resistant steels, steels that have better high temperature strength than conventional steels.

Chapter 10 is concerned with the development and use of fire engineering computer software, including two types of software originally developed by SCI to model respectively the moment capacity and temperature development in fire of floor beams. The first type of programme is used to calculate the moment capacity at elevated temperatures for slim floor beams and conventional composite I-beam floor with fire protection, which can then be used to calculate the fire resistance. The second type of programme, TFIRE, is used to model the heat transfer and the temperature development in Slimflor beams with intumescent coating protection.

## References

- Abe F (2001) Creep rates and strengthening mechanisms in tungsten-strengthened 9Cr steels. *Mater Sci Eng A* 319–321:770–773. doi:[10.1016/S0921-5093\(00\)02002-5](https://doi.org/10.1016/S0921-5093(00)02002-5)
- Abe F (2004) Coarsening behavior of lath and its effect on creep rates in tempered martensitic 9Cr-W steels. *Mater Sci Eng A* 387–389:565–569. doi:[10.1016/j.msea.2004.01.057](https://doi.org/10.1016/j.msea.2004.01.057)
- Abe F, Semba H, Sakuraya T (2007a) Effect of boron on microstructure and creep deformation behavior of tempered martensitic 9Cr steel. *Mater Sci Forum* 539–543:2982–2987
- Abe F, Taneike M, Sawada K (2007b) Alloy design of creep resistant 9Cr steel using a dispersion of nano-sized carbonitrides. *Int J Press Vessels Pip* 84:3–12. doi:[10.1016/j.ijpvp.2006.09.003](https://doi.org/10.1016/j.ijpvp.2006.09.003)
- Asahi H, Hara T, Sugiyama M, Maruyama N, Terada Y, Tamehiro H, Koyama K, Ohkita S, Morimoto H (2004a) Development of plate and seam welding technology for X120 linepipe. *Int J Offshore Polar Eng* 14:11–17
- Asahi H, Tsuru E, Hara T, Sugiyama M, Terada Y, Shinada H, Ohkita S, Morimoto H, Doi N, Murata M, Miyazaki H, Yamashita E, Yoshida T, Ayukawa N, Akasaki H, Macia ML, Petersen CW, Koo JY (2004b) Pipe production technology and properties of X120 linepipe. *Int J Offshore Polar Eng* 14:36–41
- Baluc N (2009) Material degradation under DEMO relevant neutron fluences. *Phys Scr* 2009:014004. doi:[10.1088/0031-8949/2009/T138/014004](https://doi.org/10.1088/0031-8949/2009/T138/014004)

- Baluc N, Abe K, Boutard JL, Chernov VM, Diegele E, Jitsukawa S, Kimura A, Klueh RL, Kohyama A, Kurtz RJ, Lässer R, Matsui H, Möslang A, Muroga T, Odette GR, Tran MQ, van der Schaaf B, Wu Y, Yu J, Zinkle SJ (2007a) Status of R&D activities on materials for fusion power reactors. *Nucl Fusion* 47:S696–S717. doi:[10.1088/0029-5515/47/10/S18](https://doi.org/10.1088/0029-5515/47/10/S18)
- Baluc N, Gelles DS, Jitsukawa S, Kimura A, Klueh RL, Odette GR, van der Schaaf B, Yu J (2007b) Status of reduced activation ferritic/martensitic steel development. *J Nucl Mater* 367–370:33–41. doi:[10.1016/j.jnucmat.2007.03.036](https://doi.org/10.1016/j.jnucmat.2007.03.036)
- Chen Y, Hu K (2008) Optimal design of steel portal frames based on genetic algorithms. *Front Archit Civ Eng China* 2:318–322. doi:[10.1007/s11709-008-0055-1](https://doi.org/10.1007/s11709-008-0055-1)
- Cui J, Kim IS, Kang CY, Miyahara K (2001) Creep stress effect on the precipitation behavior of Laves phase in Fe-10% Cr-6% W alloys. *ISIJ Int* 41:368–371. doi:[10.2355/isijinternational.41.368](https://doi.org/10.2355/isijinternational.41.368)
- Danielsen HK, Hald J (2004) Z-phase in 9–12%Cr steels. In: Viswanathan R, Gandy D, Coleman K (eds) *Proceedings of the 4th International Conference on Advances in Materials Technology for Fossil Power Plants*. ASM International, Materials Park, OH, pp 999–1012
- Danielsen HK, Hald J (2009) Tantalum-containing Z-phase in 12%Cr martensitic steels. *Scr Mater* 60:811–813. doi:[10.1016/j.scriptamat.2009.01.025](https://doi.org/10.1016/j.scriptamat.2009.01.025)
- Deb K (2001) *Multi-objective optimization using evolutionary algorithms*. Wiley, Chichester
- Deb K, Gulati S (2001) Design of truss-structures for minimum weight using genetic algorithms. *Finite Elem Anal Des* 37:447–465. doi:[10.1016/S0168-874X\(00\)00057-3](https://doi.org/10.1016/S0168-874X(00)00057-3)
- de Carlan Y, Muruganath M, Sourmail T, Bhadeshia HKDH (2004) Design of new Fe-9CrWV reduced-activation martensitic steels for creep properties at 650 °C. *J Nucl Mater* 329–333:238–242. doi:[10.1016/j.jnucmat.2004.04.017](https://doi.org/10.1016/j.jnucmat.2004.04.017)
- de Castro V, Leguey T, Muñoz A, Monge MA, Fernández P, Lancha AM, Pareja R (2007) Mechanical and microstructural behaviour of Y<sub>2</sub>O<sub>3</sub> ODS EUROFER 97. *J Nucl Mater* 367–370:196–201. doi:[10.1016/j.jnucmat.2007.03.146](https://doi.org/10.1016/j.jnucmat.2007.03.146)
- Fairchild DP, Macia ML, Bangaru NV, Koo JY (2004) Girth welding development for X 120 linepipe. *Int J Offshore Polar Eng* 14:18–28
- Gero MBP, García AB, del Coz Díaz JJ (2005) A modified elitist genetic algorithm applied to the design optimization of complex steel structures. *J Constr Steel Res* 61:265–280. doi:[10.1016/j.jcsr.2004.07.007](https://doi.org/10.1016/j.jcsr.2004.07.007)
- Gero MBP, García AB, del Coz Díaz JJ (2006) Design optimization of 3D steel structures: genetic algorithms vs. classical techniques. *J Constr Steel Res* 62:1303–1309. doi:[10.1016/j.jcsr.2006.02.005](https://doi.org/10.1016/j.jcsr.2006.02.005)
- Ghassemi-Armaki H, Chen RP, Maruyama K, Yoshizawa M, Igarashi M (2009) Static recovery of tempered lath martensite microstructures during long-term aging in 9–12% Cr heat resistant steels. *Mater Lett* 63:2423–2425. doi:[10.1016/j.matlet.2009.08.024](https://doi.org/10.1016/j.matlet.2009.08.024)
- Golpayegani A, Andrés HO, Danielsen H, Hald J (2008) A study on Z-phase nucleation in martensitic chromium steels. *Mater Sci Eng A* 489:310–318. doi:[10.1016/j.msea.2007.12.022](https://doi.org/10.1016/j.msea.2007.12.022)
- Guo W, Dong H, Lu M, Zhao X (2002) The coupled effects of thickness and delamination on cracking resistance of X70 pipeline steel. *Int J Pressure Vessels Pip* 79:403–412. doi:[10.1016/S0308-0161\(02\)00039-X](https://doi.org/10.1016/S0308-0161(02)00039-X)
- Guo Z, Sha W, Vaumousse D (2003) Microstructural evolution in a PH13-8 stainless steel after ageing. *Acta Mater* 51:101–116. doi:[10.1016/S1359-6454\(02\)00353-1](https://doi.org/10.1016/S1359-6454(02)00353-1)
- Guo Z, Sha W (2004a) Kinetics of ferrite to Widmanstätten austenite transformation in a high-strength low-alloy steel revisited. *Z Metallkd* 95:718–723
- Guo Z, Sha W (2004b) Comments on small-angle neutron scattering analysis of the precipitation behaviour in a maraging steel by Staron, Jammig, Leitner, Ebner & Clemens (2003). *J Appl Crystallogr* 37:325–326. doi:[10.1107/S0021889803028127](https://doi.org/10.1107/S0021889803028127)
- Guo Z, Sha W, Li D (2004) Quantification of phase transformation kinetics of 18 wt.% Ni C250 maraging steel. *Mater Sci Eng A* 373:10–20. doi:[10.1016/j.msea.2004.01.040](https://doi.org/10.1016/j.msea.2004.01.040)
- Gustafson Å, Ågren J (2001) Possible effect of Co on coarsening of M<sub>23</sub>C<sub>6</sub> carbide and Orowan stress in a 9% Cr steel. *ISIJ Int* 41:356–360. doi:[10.2355/isijinternational.41.356](https://doi.org/10.2355/isijinternational.41.356)
- Hernández S, Fontán AN, Perezán JC, Loscos P (2005) Design optimization of steel portal frames. *Adv Eng Softw* 36:626–633. doi:[10.1016/j.advengsoft.2005.03.006](https://doi.org/10.1016/j.advengsoft.2005.03.006)

- Howe AA (2000) Ultrafine grained steels: industrial prospects. *Mater Sci Technol* 16:1264–1266. doi:[10.1179/026708300101507488](https://doi.org/10.1179/026708300101507488)
- Issa HK, Mohammad FA (2010) Effect of mutation schemes on convergence to optimum design of steel frames. *J Constr Steel Res* 66:954–961. doi:[10.1016/j.jcsr.2010.02.002](https://doi.org/10.1016/j.jcsr.2010.02.002)
- Jitsukawa S, Tamura M, van der Schaaf B, Klueh RL, Alamo A, Petersen C, Schirra M, Spaetig P, Odette GR, Tavassoli AA, Shiba K, Kohyama A, Kimura A (2002) Development of an extensive database of mechanical and physical properties for reduced-activation martensitic steel F82H. *J Nucl Mater* 307–311:179–186. doi:[10.1016/S0022-3115\(02\)01075-9](https://doi.org/10.1016/S0022-3115(02)01075-9)
- Jitsukawa S, Suzuki K, Okubo N, Ando M, Shiba K (2009) Irradiation effects on reduced activation ferritic/martensitic steels—tensile, impact, fatigue properties and modelling. *Nucl Fusion* 49:115006. doi:[10.1088/0029-5515/49/11/115006](https://doi.org/10.1088/0029-5515/49/11/115006)
- Kameshki E, Saka MP (2001) Optimum design of nonlinear steel frames with semi-rigid connections using a genetic algorithm. *Comput Struct* 79:1593–1604. doi:[10.1016/S0045-7949\(01\)00035-9](https://doi.org/10.1016/S0045-7949(01)00035-9)
- Kim YM, Kim SK, Lim YJ, Kim NJ (2002) Effect of microstructure on the yield ratio and low temperature toughness of linepipe steels. *ISIJ Int* 42:1571–1577. doi:[10.2355/isijinternational.42.1571](https://doi.org/10.2355/isijinternational.42.1571)
- Kimura Y, Inoue T, Yin F, Sitdikov O, Tsuzaki K (2007) Toughening of a 1500 MPa class steel through formation of an ultrafine fibrous grain structure. *Scr Mater* 57:465–468. doi:[10.1016/j.scriptamat.2007.05.039](https://doi.org/10.1016/j.scriptamat.2007.05.039)
- Kimura K, Toda Y, Kushima H, Sawada K (2010) Creep strength of high chromium steel with ferrite matrix. *Int J Press Vessels Pip* 87:282–288. doi:[10.1016/j.ijpvp.2010.03.016](https://doi.org/10.1016/j.ijpvp.2010.03.016)
- Klimenkov M, Lindau R, Möslang A (2009) New insights into the structure of ODS particles in the ODS-Eurofer alloy. *J Nucl Mater* 386–388:553–556. doi:[10.1016/j.jnucmat.2008.12.174](https://doi.org/10.1016/j.jnucmat.2008.12.174)
- Klueh RL (2008) Reduced-activation steels: future development for improved creep strength. *J Nucl Mater* 378:159–166. doi:[10.1016/j.jnucmat.2008.05.010](https://doi.org/10.1016/j.jnucmat.2008.05.010)
- Klueh RL, Cheng ET, Grossbeck ML, Bloom EE (2000) Impurity effects on reduced-activation ferritic steels developed for fusion applications. *J Nucl Mater* 280:353–359. doi:[10.1016/S0022-3115\(00\)00060-X](https://doi.org/10.1016/S0022-3115(00)00060-X)
- Klueh RL, Gelles DS, Jitsukawa S, Kimura A, Odette GR, van der Schaaf B, Victoria M (2002) Ferritic/martensitic steels—overview of recent results. *J Nucl Mater* 307–311:455–465. doi:[10.1016/S0022-3115\(02\)01082-6](https://doi.org/10.1016/S0022-3115(02)01082-6)
- Klueh RL, Hashimoto N, Maziasz PJ (2007) New nano-particle-strengthened ferritic/martensitic steels by conventional thermo-mechanical treatment. *J Nucl Mater* 367–370:48–53. doi:[10.1016/j.jnucmat.2007.03.001](https://doi.org/10.1016/j.jnucmat.2007.03.001)
- Koo JY, Luton MJ, Bangaru NV, Petkovic RA, Fairchild DP, Petersen CW, Asahi H, Hara T, Terada Y, Sugiyama M, Tamehiro H, Komizo Y, Okaguchi S, Hamada M, Yamamoto A, Takeuchi I (2004) Metallurgical design of ultra high-strength steels for gas pipelines. *Int J Offshore Polar Eng* 14:2–10
- Kurtz RJ, Alamo A, Lucon E, Huang Q, Jitsukawa S, Kimura A, Klueh RL, Odette GR, Petersen C, Sokolov MA, Spätig P, Rensman JW (2009) Recent progress toward development of reduced activation ferritic/martensitic steels for fusion structural applications. *J Nucl Mater* 386–388:411–417. doi:[10.1016/j.jnucmat.2008.12.323](https://doi.org/10.1016/j.jnucmat.2008.12.323)
- Lee JS, Armaki HG, Maruyama K, Maruki T, Asahi H (2006) Causes of breakdown of creep strength in 9Cr-1.8W-0.5Mo-VNb steel. *Mater Sci Eng A* 428:270–275. doi:[10.1016/j.msea.2006.05.010](https://doi.org/10.1016/j.msea.2006.05.010)
- Leinonen JI (2001) Processing steel for higher strength. *Adv Mater Process* 159(11):31–33
- Leitner H, Schober M, Schnitzer R (2010) Splitting phenomenon in the precipitation evolution in an Fe-Ni-Al-Ti-Cr stainless steel. *Acta Mater* 58:1261–1269. doi:[10.1016/j.actamat.2009.10.030](https://doi.org/10.1016/j.actamat.2009.10.030)
- Li PJ, Xiong YH, Liu SX, Zeng DB (2003) Electron theory study on mechanism of action of cobalt in Fe-Co-Cr based high-alloy steel. *Chin Sci Bull* 48:208–210
- Lim JBP, Nethercot DA (2002) Design and development of a general cold-formed steel portal framing system. *Struct Eng* 80(21):31–40
- Lindau R, Möslang A, Rieth M, Klimiankou M, Materna-Morris E, Alamo A, Tavassoli AAF, Cayron C, Lancha AM, Fernandez P, Baluc N, Schäublin R, Diegele E, Filacchioni G, Rensman JW, van der Schaaf B, Lucon E, Dietz W (2005) Present development status of

- EUROFER and ODS-EUROFER for application in blanket concepts. *Fusion Eng Des* 75–79:989–996. doi:[10.1016/j.fusengdes.2005.06.186](https://doi.org/10.1016/j.fusengdes.2005.06.186)
- Maruyama K, Sawada K, Koike J (2001) Strengthening mechanisms of creep resistant tempered martensitic steel. *ISIJ Int* 41:641–653. doi:[10.2355/isijinternational.41.641](https://doi.org/10.2355/isijinternational.41.641)
- Masuyama F (2001) History of power plants and progress in heat resistant steels. *ISIJ Int* 41:612–625. doi:[10.2355/isijinternational.41.612](https://doi.org/10.2355/isijinternational.41.612)
- Miyata K, Sawaragi Y (2001) Effect of Mo and W on the phase stability of precipitates in low Cr heat resistant steels. *ISIJ Int* 41:281–289. doi:[10.2355/isijinternational.41.281](https://doi.org/10.2355/isijinternational.41.281)
- Morris JW, Krenn CR, Guo Z (2000) 19th ASM Heat Treating Society conference and exposition including steel heat treating in the new millenium: an international symposium in honor of Professor George Krauss. ASM International, Materials Park, pp 526–535
- Olier P, Bougault A, Alamo A, de Carlan Y (2009) Effects of the forming processes and  $Y_2O_3$  content on ODS-Eurofer mechanical properties. *J Nucl Mater* 386–388:561–563. doi:[10.1016/j.jnucmat.2008.12.177](https://doi.org/10.1016/j.jnucmat.2008.12.177)
- Otárola T, Hollner S, Bonnefois B, Anglada M, Coudreuse L, Mateo A (2005) Embrittlement of a superduplex stainless steel in the range of 550–700 °C. *Eng Fail Anal* 12:930–941. doi:[10.1016/j.engfailanal.2004.12.022](https://doi.org/10.1016/j.engfailanal.2004.12.022)
- Pozuelo M, Carreño F, Ruano O (2006) A delamination effect on the impact toughness of an ultrahigh carbon-mild steel laminate composite. *Compos Sci Technol* 66:2671–2676. doi:[10.1016/j.compscitech.2006.03.018](https://doi.org/10.1016/j.compscitech.2006.03.018)
- Priestner R, Ibraheem AK (2000) Processing of steel for ultrafine ferrite grain structures. *Mater Sci Technol* 16:1267–1272. doi:[10.1179/026708300101507497](https://doi.org/10.1179/026708300101507497)
- Rhodes J, Burns R (2006) Development of a portal frame system on the basis of component testing. In: Proceedings of the 18th international specialty conference on cold-formed steel structures, University of Missouri-Rolla, Missouri, pp 367–385
- Ryu SH, Lee YS, Kong BO, Kim JT, Kwak DH, Nam SW et al (2006) In: Proceedings of the 3rd international conference on advanced structural steels. The Korean Institute of Metals and Materials, pp 563–569
- Saka MP (2003) Optimum design of pitched roof steel frames with haunched rafters by genetic algorithm. *Comput Struct* 81:1967–1978. doi:[10.1016/S0045-7949\(03\)00216-5](https://doi.org/10.1016/S0045-7949(03)00216-5)
- Saroja S, Dasgupta A, Divakar R, Raju S, Mohandas E, Vijayalakshmi M, Rao KBS, Raj B (2011) Development and characterization of advanced 9Cr ferritic/martensitic steels for fission and fusion reactors. *J Nucl Mater* 409:131–139. doi:[10.1016/j.jnucmat.2010.09.022](https://doi.org/10.1016/j.jnucmat.2010.09.022)
- Sawada K, Kubo K, Abe F (2001) Creep behavior and stability of MX precipitates at high temperature in 9Cr-0.5Mo-1.8W-VNb steel. *Mater Sci Eng A* 319–321:784–787. doi:[10.1016/S0921-5093\(01\)00973-X](https://doi.org/10.1016/S0921-5093(01)00973-X)
- Sawada K, Taneike M, Kimura K, Abe F (2004) Effect of nitrogen content on microstructural aspects and creep behavior in extremely low carbon 9Cr heat-resistant steel. *ISIJ Int* 44:1243–1249. doi:[10.2355/isijinternational.44.1243](https://doi.org/10.2355/isijinternational.44.1243)
- Sawada K, Kushima H, Kimura K (2006a) Z-phase formation during creep and aging in 9–12% Cr heat resistant steels. *ISIJ Int* 46:769–775. doi:[10.2355/isijinternational.46.769](https://doi.org/10.2355/isijinternational.46.769)
- Sawada K, Kushima H, Kimura K, Tabuchi M (2006b) Creep strength degradation by Z phase formation in 9-12%Cr heat resistant steels. In: Proceedings of the 3rd international conference on advanced structural steels. The Korean Institute of Metals and Materials, pp 532–537
- Sawada K, Kushima H, Kimura K, Tabuchi M (2007) TTP diagrams of Z phase in 9–12% Cr heat-resistant steels. *ISIJ Int* 47:733–739. doi:[10.2355/isijinternational.47.733](https://doi.org/10.2355/isijinternational.47.733)
- Schaeublin R, Leguey T, Spätig P, Baluc N, Victoria M (2002) Microstructure and mechanical properties of two ODS ferritic/martensitic steels. *J Nucl Mater* 307–311:778–782. doi:[10.1016/S0022-3115\(02\)01193-5](https://doi.org/10.1016/S0022-3115(02)01193-5)
- Sha W, Guo Z (2009) Maraging steels: modelling of microstructure, properties and applications. Woodhead Publishing, Cambridge. doi:[10.1533/9781845696931](https://doi.org/10.1533/9781845696931)
- Sha W, Kirby BR, Kelly FS (2001) The behaviour of structural steels at elevated temperatures and the design of fire resistant steels. *Mater Trans* 42:1913–1927

- Shen YZ, Kim SH, Cho HD, Han CH, Ryu WS (2009) Precipitate phases of a ferritic/martensitic 9% Cr steel for nuclear power reactors. *Nucl Eng Des* 239:648–654. doi:[10.1016/j.nucengdes.2008.12.018](https://doi.org/10.1016/j.nucengdes.2008.12.018)
- Silva MC, Hippert Jr E, Ruggieri C (2005) In: Proceedings of ASME pressure vessels and piping conference. ASME, Denver, pp 87–94
- Song R, Ponge D, Raabe D (2005) Mechanical properties of an ultrafine grained C-Mn steel processed by warm deformation and annealing. *Acta Mater* 53:4881–4892. doi:[10.1016/j.actamat.2005.07.009](https://doi.org/10.1016/j.actamat.2005.07.009)
- Song R, Ponge D, Raabe D, Speer JG, Matlock DK (2006) Overview of processing, microstructure and mechanical properties of ultrafine grained bcc steels. *Mater Sci Eng A* 441:1–17. doi:[10.1016/j.msea.2006.08.095](https://doi.org/10.1016/j.msea.2006.08.095)
- Taneike M, Abe F, Sawada K (2003) Creep-strengthening of steel at high temperatures using nano-sized carbonitride dispersions. *Nature* 424:294–296. doi:[10.1038/nature01740](https://doi.org/10.1038/nature01740)
- Taneike M, Sawada K, Abe F (2004) Effect of carbon concentration on precipitation behavior of  $M_{23}C_6$  carbides and MX carbonitrides in martensitic 9Cr steel during heat treatment. *Metall Mater Trans A* 35A:1255–1262. doi:[10.1007/s11661-004-0299-x](https://doi.org/10.1007/s11661-004-0299-x)
- Toda Y, Seki K, Kimura K, Abe F (2003) Effects of W and Co on long-term creep strength of precipitation strengthened 15Cr ferritic heat resistant steels. *ISIJ Int* 43:112–118. doi:[10.2355/isijinternational.43.112](https://doi.org/10.2355/isijinternational.43.112)
- Toda Y, Tohyama H, Kushima H, Kimura K, Abe F (2005) Improvement in creep strength of precipitation strengthened 15Cr ferritic steel by controlling carbon and nitrogen contents. *JSME Int J Ser A* 48:35–40. doi:[10.1299/jsmea.48.35](https://doi.org/10.1299/jsmea.48.35)
- Toropov VV, Mahfouz SY (2001) Design optimization of structural steelwork using a genetic algorithm, FEM and a system of design rules. *Eng Comput* 18:437–460. doi:[10.1108/02644400110387118](https://doi.org/10.1108/02644400110387118)
- Tsuji N, Okuno S, Koizumi Y, Minamino Y (2004) Toughness of ultrafine grained ferritic steels fabricated by ARB and annealing process. *Mater Trans* 45:2272–2281. doi:[10.2320/matertrans.45.2272](https://doi.org/10.2320/matertrans.45.2272)
- van der Schaaf B, Gelles DS, Jitsukawa S, Kimura A, Klueh RL, Möslang A, Odette GR (2000) Progress and critical issues of reduced activation ferritic/martensitic steel development. *J Nucl Mater* 283–287:52–59. doi:[10.1016/S0022-3115\(00\)00220-8](https://doi.org/10.1016/S0022-3115(00)00220-8)
- Verdeja JI, Asensio J, Pero-Sanz JA (2003) Texture, formability, lamellar tearing and HIC susceptibility of ferritic and low-carbon HSLA steels. *Mater Charact* 50:81–86. doi:[10.1016/S1044-5803\(03\)00106-2](https://doi.org/10.1016/S1044-5803(03)00106-2)
- Wallin K (2001) Upper shelf energy normalisation for sub-sized Charpy-V specimens. *Int J Pressure Vessels Pip* 78:463–470. doi:[10.1016/S0308-0161\(01\)00063-1](https://doi.org/10.1016/S0308-0161(01)00063-1)
- Wang W, Shan Y, Yang K (2009a) Study of high strength pipeline steels with different microstructures. *Mater Sci Eng A* 502:38–44. doi:[10.1016/j.msea.2008.10.042](https://doi.org/10.1016/j.msea.2008.10.042)
- Wang Y, Mayer KH, Scholz A, Berger C, Chilukuru H, Durst K, Blum W (2009b) Development of new 11%Cr heat resistant ferritic steels with enhanced creep resistance for steam power plants with operating steam temperatures up to 650 °C. *Mater Sci Eng A* 510–511:180–184. doi:[10.1016/j.msea.2008.04.116](https://doi.org/10.1016/j.msea.2008.04.116)
- Weisenburger A, Heinzl A, Müller G, Muscher H, Rousanov A (2008) T91 cladding tubes with and without modified FeCrAlY coatings exposed in LBE at different flow, stress and temperature conditions. *J Nucl Mater* 376:274–281. doi:[10.1016/j.jnucmat.2008.02.026](https://doi.org/10.1016/j.jnucmat.2008.02.026)
- Wong CPC, Salavy JF, Kim Y, Kirillov I, Kumar ER, Morley NB, Tanaka S, Wu YC (2008) Overview of liquid metal TBM concepts and programs. *Fusion Eng Des* 83:850–857. doi:[10.1016/j.fusengdes.2008.06.040](https://doi.org/10.1016/j.fusengdes.2008.06.040)
- Yamada K, Igarashi M, Muneki S, Abe F (2003) Effect of Co addition on microstructure in high Cr ferritic steels. *ISIJ Int* 43:1438–1443. doi:[10.2355/isijinternational.43.1438](https://doi.org/10.2355/isijinternational.43.1438)
- Yang M, Chao YJ, Li X, Tan J (2008a) Splitting in dual-phase 590 high strength steel plates: Part I. Mechanisms. *Mater Sci Eng A* 497:451–461. doi:[10.1016/j.msea.2008.07.067](https://doi.org/10.1016/j.msea.2008.07.067)
- Yang M, Chao YJ, Li X, Immel D, Tan J (2008b) Splitting in dual-phase 590 high strength steel plates: Part II. Quantitative analysis and its effect on Charpy impact energy. *Mater Sci Eng A* 497:462–470. doi:[10.1016/j.msea.2008.07.066](https://doi.org/10.1016/j.msea.2008.07.066)

- Yin F, Jung W (2009) Nanosized MX precipitates in ultra-low-carbon ferritic/martensitic heat-resistant steels. *Metall Mater Trans A* 40A:302–309. doi:[10.1007/s11661-008-9716-x](https://doi.org/10.1007/s11661-008-9716-x)
- Yin F, Jung W, Chung S (2007) Microstructure and creep rupture characteristics of an ultra-low carbon ferritic/martensitic heat-resistant steel. *Scr Mater* 57:469–472. doi:[10.1016/j.scriptamat.2007.05.034](https://doi.org/10.1016/j.scriptamat.2007.05.034)
- Yong Q (2006) *The second phase in steels*. Metallurgical Industry Press, Beijing
- Yoshizawa M, Igarashi M (2007) Long-term creep deformation characteristics of advanced ferritic steels for USC power plants. *Int J Press Vessels Pip* 84:37–43. doi:[10.1016/j.ijpvp.2006.09.005](https://doi.org/10.1016/j.ijpvp.2006.09.005)
- Yu G, Nita N, Baluc N (2005) Thermal creep behaviour of the EUROFER 97 RAFM steel and two European ODS EUROFER 97 steels. *Fusion Eng Des* 75–79:1037–1041. doi:[10.1016/j.fusengdes.2005.06.311](https://doi.org/10.1016/j.fusengdes.2005.06.311)
- Zhao MC, Shan YY, Xiao FR, Yang K, Li YH (2002) Investigation on the H<sub>2</sub>S-resistant behaviors of acicular ferrite and ultrafine ferrite. *Mater Lett* 57:141–145. doi:[10.1016/S0167-577X\(02\)00720-6](https://doi.org/10.1016/S0167-577X(02)00720-6)
- Zhao X, Jing TF, Gao YW, Qiao GY, Zhou JF, Wang W (2005) Annealing behavior of nano-layered steel produced by heavy cold-rolling of lath martensite. *Mater Sci Eng A* 397:117–121. doi:[10.1016/j.msea.2005.02.007](https://doi.org/10.1016/j.msea.2005.02.007)